Ether flow through a drainhole: A particle model in general relativity

Homer G. Ellis

Articles you may be interested in
Two Phase Flow Modelling for Low Concentration Spherical Particle Motion Through a Newtonian Fluid
AIP Conf. Proc. **1168**, 673 (2009); 10.1063/1.3241554

Particle-in-cell modeling of magnetized argon plasma flow through small mechanical apertures
Phys. Plasmas **16**, 053501 (2009); 10.1063/1.3119902

Asymptotic model of the inertial migration of particles in a dilute suspension flow through the entry region of a channel
Phys. Fluids **20**, 123301 (2008); 10.1063/1.3032909

Errata: Ether flow through a drainhole: A particle model in general relativity
J. Math. Phys. **15**, 520 (1974); 10.1063/1.1666675

Conserved Particle Structures in General Relativity
J. Math. Phys. **12**, 308 (1971); 10.1063/1.1665593

Ether flow through a drainhole: A particle model in general relativity

Homer G. Ellis

Department of Mathematics, University of Colorado, Boulder, Colorado 80302

The Schwarzschild manifold of general relativity theory is unsatisfactory as a particle model because the singularity at the origin makes it geodesically incomplete. A coupling of the geometry of space–time to a scalar field ϕ produces in its stead a static, spherically symmetric, geodesically complete, horizonless space–time manifold with a topological hole, termed a drainhole, in its center. The coupling is $R_{\mu\nu} = 2\phi_{,\mu}\phi_{,\nu}$; its polarity is reversed from the usual to allow both the negative curvatures found in the drainhole and the completeness of the geodesics. The scalar field satisfies the scalar wave equation $\Box\phi = 0$ and has finite total energy whose magnitude, expressed as a length, is comparable to the drainhole radius. On one side of the drainhole the manifold is asymptotic to a Schwarzschild manifold with positive mass parameter m, on the other to a Schwarzschild manifold with negative mass parameter $\bar{m}$, and $-\bar{m} > m$. The two-sided particle thus modeled attracts matter on the one side and, with greater strength, repels it on the other. If m is one proton mass, then $-\bar{m}/m \simeq 1 + 10^{-19}$ or $1 + 10^{-39}$, according as the drainhole radius is close to 10^{-33}cm or close to 10^{-13} cm; the ratios of total scalar field energy to m in these instances are 10^{19} and 10^{39}. A radially directed vector field which presents itself is interpreted, for purposes of conceptualization, as the velocity of a flowing "substantial ether" whose nonrigid motions manifest themselves as gravitational phenomena. When the ether is at rest, the two-sided particle has no mass on either side, but the drainhole remains open and is able to trap test particles for any finite length of time, then release them without ever accelerating them; some it can trap for all time without accelerating them. This massless, chargeless, spinless particle can, if disturbed, dematerialize into a scalar-field wave propagating at the wave speed characteristic of the space–time manifold.

I. INTRODUCTION

Ever since Schwarzschild presented his spherically symmetric solution of the Einstein vacuum gravitational field equations,[1] it has been a common practice to think of space–time manifolds with "point singularities" as the most appropriate models for mass particles within general relativity theory. Such manifolds, however, are unsatisfactory as models because they are not geodesically complete, failing to provide complete histories for test particles and light rays that encounter the singularities. Einstein and Rosen attempted to do away with the Schwarzschild point singularity by connecting together two Schwarzschild exteriors by a "bridge" at the Schwarzschild horizon.[2] They hoped by thus picturing elementary particles as topological holes in space to explain the atomistic character of matter. They also held out the possibility of explaining quantum phenomena in the same way. The manifold that they constructed, however, not only carried a degenerate metric, which they were prepared to accept, it also suffered the defect of being geodesically incomplete. In cutting away the Schwarzschild interiors they had taken portions of geodesics whose remaining parts they had not subsequently pieced out to completeness.

In more recent times Kruskal has shown,[3] and Fronsdal independently has shown,[4] that the maximal analytic extension of the Schwarzschild manifold has in it a hole, associated with the Schwarzschild horizon, that is topologically but not metrically like the hole in the Einstein-Rosen manifold. This hole Wheeler has termed a "wormhole"[5]; it connects the two Schwarzschild exteriors found in the maximal analytic extension. Some of the geodesics that in the Schwarzschild manifold terminate abruptly at the horizon are, in the maximal extension, completed through the wormhole. However, there are others in the extended manifold that arrive at one of its two point singularities without having exhausted their affine parameters. Hence the maximal analytic extension is geodesically incomplete because of the point singularities.

To get a geodesically complete space–time manifold with a hole in it by which to represent a mass particle, one must find a way to force open the Schwarzschild singularity and there to connect on an additional chunk of space–time, taking care to preserve those features of the original manifold that bring it into agreement with the observable properties of the mass particle. The main object of this writing is to show how that may be done. The hole that replaces the singularity will differ in important respects from the Einsten–Rosen bridge and from the Kruskal–Fronsdal wormhole. At the risk of superadding coinage I shall refer to this hole as a "drainhole." The rationale for this name is that on the space–time manifold containing the hole there is a vector field that can be interpreted as a velocity field for an "ether" draining through the hole. The existence of the hole permits this ether to be conserved in the sense that its streamlines, which are timelike geodesics, never abruptly terminate. It is intriguing that the manifolds that contain one of these drainholes have among them not only reasonable models of mass particles, but also novel models of massless particles with the ability to hold test particles in close orbit for arbitrary lengths of time without accelerating them. These particles, both the massive and the massless, could serve as nuclear glue.

It is clear that these drainhole manifolds, if spherically symmetric, cannot satisfy Einstein's vacuum field equations. Indeed, according to a theorem of Birkhoff, the only spherically symmetric space–time manifold that does so is Schwarzschild's.[6] A "plumber's friend" is needed to open up the Schwarzschild singularity with. The device that will be used is a scalar field. This field ϕ will satisfy the scalar wave equation $\Box\phi = 0$ and will be coupled to the metric of the space–time manifold through the field equations $R_{\mu\nu} = 2\phi_{,\mu}\phi_{,\nu}$, the $R_{\mu\nu}$ being the components of the Ricci tensor field. The polarity of the coupling, which is opposite to the customarily accepted polarity, will be seen to be fixed by the requirement that these field equations

have a static, spherically symmetric, and geodesically complete solution manifold.

It will be convenient to begin with a discussion of a generalized drainhole line element and the geometrical and physical entities that can be associated with it, without at first imposing the field equations (Secs. II–V). After an argument to motivate the choice of field equations (Sec. VI), there will come a description of all their solution manifolds that carry such a line element (Sec. VII), a proof that some of these manifolds are geodesically complete and a description of their geodesics (Sec. VIII), and a final discussion, devoted mainly to the choice of coupling polarity in the field equations and including a proof that every static and spherically symmetric line element can be brought into the adopted form (Sec. IX). The computational framework to be used will be found outlined in the Appendix.

II. THE DRAINHOLE LINE ELEMENT

When referred to a certain nicely adapted coordinate system, the general line element in question takes the spherically symmetric form

$$d\tau^2 = dt^2 - [d\rho - f(\rho)dt]^2 - r^2(\rho)[d\vartheta^2 + (\sin\vartheta)^2 d\varphi^2]$$

$$= dt^2 - [d\rho - f(\rho)dt]^2 - r^2(\rho)d\Omega^2. \quad (1)$$

The function f and the nonnegative function r are to be determined by the field equations. The coordinate ranges are given by

$$-\infty < t < \infty, \ -\infty < \rho < \infty, \ 0 < \vartheta < \pi, \ -\pi < \varphi < \pi, \quad (2)$$

and the additional stipulation that $\rho \in \text{dmn} f \cap \text{dmn} r - r^{-1}(0)$. The determinant of the metric tensor in this coordinate system is $-[r^2(\rho)\sin\vartheta]^2$; it is, as a result, independent of f. Because $r^{-1}(0)$ is excluded from the range of ρ, the line element is regular for all values of the coordinates.

Once the functions f and r have been specified, the line element may be considered to lie upon a manifold $\mathfrak{M}$ that is almost globally coordinatized by the coordinate system $[t, \rho, \vartheta, \varphi]$, the points without coordinates being those at which $\lim\inf r(\rho) = 0$, $\lim\vartheta = 0$ or π, or $\lim\varphi = \pm\pi$. Because the metric coefficients in Eq. (1) are independent of t, all translations of $\mathfrak{M}$ along the t coordinate curves are isometries; hence $\partial/\partial t$ is a Killing vector field. Inasmuch as $|\partial/\partial t|^2 = 1 - f^2$, $\partial/\partial t$ is timelike, null, or spacelike according as $f^2 < 1$, $f^2 = 1$, or $f^2 > 1$. Consequently, those regions of $\mathfrak{M}$ where $f^2 < 1$ are stationary. Because $2f(\rho)d\rho dt$ is the only cross term in $\mathfrak{M}$'s line element, $\partial/\partial t$ is not everywhere orthogonal to the hypersurfaces of constant t unless $f = 0$, in which event $\mathfrak{M}$ is static. Actually, $\mathfrak{M}$ is static wherever $f^2 < 1$. This is established in Sec. V, where it is shown that $\partial/\partial t$ is orthogonal to other hypersurfaces.

Let Σ_t denote the cross section of $\mathfrak{M}$ on which the time coordinate has the constant value t.[7] Σ_t is spacelike and inherits from $\mathfrak{M}$ the Riemannian line element given by

$$d\sigma^2 = d\rho^2 + r^2(\rho)d\Omega^2. \quad (3)$$

If it were the case that $r(\rho) = \rho$, then this would be the line element of Euclidean 3-space E^3, cast in polar coordinates ρ, ϑ, and φ. In the general case Σ_t may be

thought of as a warped portion of E^3. The warping, caused by deviations of $r(\rho)$ from the Euclidean value ρ, does not destroy the spherical symmetry. The cross section $S_{t,\rho}$ on which the radial coordinate has the constant value ρ is simply a geometrical 2-sphere of radius $r(\rho)$. If $r(\rho)$ has a positive minimum value, then Σ_t has a central hole of that radius, it being the radius of the smallest such 2-sphere $S_{t,\rho}$ in Σ_t.

A case that will arise later has $r(\rho) = (\rho^2 + n^2)^{1/2}$, where n is a positive constant and is the radius of the hole, a particular instance of the drainhole. In this case the equatorial cross section of Σ_t, typical of all great-circle cross sections of Σ_t, may be pictured as in Fig. 1. It is isometrically embeddable in E^3 as $\{[x,y,z] \mid (x^2 + y^2)^{1/2} = n \cosh(z/n)\}$, a catenoid. Σ_t itself is congruent to $\{[x,y,z,w] \mid (x^2 + y^2 + z^2)^{1/2} = n \cosh(w/n)\}$ in E^4. Σ_t is asymptotic to E^3, in a sense that can be made precise, both as $\rho \to \infty$ and as $\rho \to -\infty$. This is primarily because, in each instance, $\lim[r(\rho)/|\rho|] = 1$.

III. THE ETHER FLOW

The vector field u on the manifold $\mathfrak{M}$, defined by

$$u = \frac{\partial}{\partial t} + f(\rho)\frac{\partial}{\partial\rho}, \quad (4)$$

has many interesting properties. To begin with, it is everywhere timelike, of unit length, and orthogonal to a cross section Σ_t. Thus it may serve as the timelike vector field in an orthonormal frame system whose spacelike vector fields are tangent to these hypersurfaces Σ_t. One such frame system is $\{e_\mu\}$ defined as follows:

$$e_0 = u = \frac{\partial}{\partial t} + f(\rho)\frac{\partial}{\partial\rho}, \ e_1 = \frac{\partial}{\partial\rho},$$

$$e_2 = \frac{1}{r(\rho)}\frac{\partial}{\partial\vartheta}, \ e_3 = \frac{1}{r(\rho)\sin\vartheta}\frac{\partial}{\partial\varphi}. \quad (5)$$

The system coframe $\{\omega^\mu\}$ dual to $\{e_\mu\}$ is given by

$$\omega^0 = dt, \ \omega^1 = d\rho - f(\rho)dt,$$

$$\omega^2 = r(\rho)d\vartheta, \ \omega^3 = r(\rho)(\sin\vartheta)d\varphi. \quad (6)$$

Determining the unique torsion-free covariant differentiation d that is consistent with the metric is made easy by the use of this orthonormal frame system. The connection forms are found to be expressed by[8]
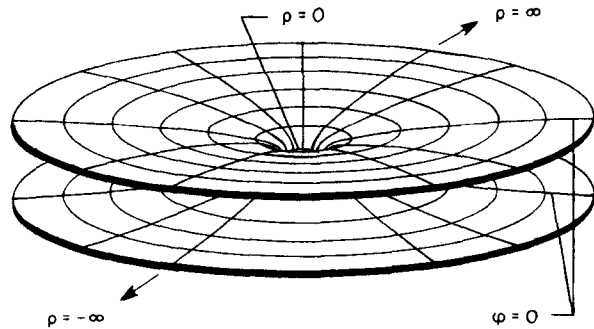

FIG. 1. The equatorial cross section of the typical spatial cross section Σ_t of the space–time manifold $\mathfrak{M}$ in a special case. The line element of this surface is given by $d\sigma^2 = d\rho^2 + (\rho^2 + n^2)d\varphi^2$. The surface is isometric to the catenoid $\{[x,y,z] \mid (x^2 + y^2)^{1/2} = n \cosh(z/n)\}$ in E^3. The radius of the central hole, where $\rho = 0$, is n. The surface is asymptotic to E^2, both as $\rho \to \infty$ and as $\rho \to -\infty$.

$$[\omega_\kappa{}^\mu] = \begin{bmatrix} 0 & f'\omega^1 & (r'/r)f\omega^2 & (r'/r)f\omega^3 \\ f'\omega^1 & 0 & (r'/r)\omega^2 & (r'/r)\omega^3 \\ (r'/r)f\omega^2 & -(r'/r)\omega^2 & 0 & [(\text{ctn}\,\vartheta)/r]\omega^3 \\ (r'/r)f\omega^3 & -(r'/r)\omega^3 & -[(\text{ctn}\,\vartheta)/r]\omega^3 & 0 \end{bmatrix} . \tag{7}$$

Because $u = e_0$,

$$du = f'(\omega^1 \otimes e_1) + (r'/r)f(\omega^2 \otimes e_2 + \omega^3 \otimes e_3) \tag{8}$$

and

$$duu = f'(\omega^1 e_0)e_1 + (r'/r)f[\omega^2 e_0)e_2 + (\omega^3 e_0)e_3] = 0. \tag{9}$$

Another property of the vector field u now becomes apparent: each of its integral paths is geodesic. If p is an integral path of u, then

$$\dot{p} = u(p) = e_0(p); \tag{10}$$

hence

$$\ddot{p} = du(p)\dot{p} = (duu)(p) = 0. \tag{11}$$

Thus p is geodesic and is parametrized by an affine parameter, which is, because $|\dot{p}|^2 = |u(p)|^2 = 1$, the proper time along p measured from some initial point. Therefore, u generates a congruence of timelike geodesics parametrized by proper time, filling up the space-time manifold $\mathfrak{M}$.

In attempting to understand gravity, I have found it useful to accept as a working hypothesis the existence of a more or less substantial "ether," pervading all of space-time. The ether that I imagine is more than a mere inert medium for the propagation of electromagnetic waves; it is a restless, flowing continuum whose internal, relative motions manifest themselves to us as gravity. Mass particles appear as sinks or sources of this flowing ether. In the case of the space-time manifold $\mathfrak{M}$ under discussion here the velocity that I associate with the ether flow is the vector field u. The geodesic property of u just now established I interpret as saying that every observer or test particle drifting with the ether, following its flow, is absolutely unaccelerated. In this sense my hypothetical ether provides a universal system of inertial observers, just as did the nineteenth-century luminiferous ether, and as must every ether worthy of the name.

It was in pursuing the consequences of this hypothesis that I became convinced of the need to replace the Schwarzschild singularity with a drainhole. Telling how to do that is the principal aim here, and I shall therefore make no effort to justify the ether-flow hypothesis.[9,10] Although henceforth I shall refer to u as "the ether flow velocity" and speak of "the ether" as if it really does exist and flow about, I shall do so not because I expect the reader to adopt this hypothesis, rather because the concepts and terminology provide an expressive and stimulating vehicle of thought that I am accustomed to using. Whether there is such an ether is a question that requires clarification if it is to be answered with confidence.

Returning now to the discussion of geodesics associated with the ether flow velocity u, let us first note that if p is any path in the manifold $\mathfrak{M}$, then, in terms of the ortho-

normal frame system $\{e_\mu\}$,

$$\dot{p} = \dot{t}e_0(p) + [\dot{\rho} - f(\rho)\dot{t}]e_1(p)$$
$$+ r(\rho)\dot{\vartheta}e_2(p) + r(\rho)(\sin\vartheta)\dot{\varphi}e_3(p), \tag{12}$$

where by abuse of notation $t, \rho, \vartheta,$ and φ stand for $t(p)$, $\rho(p), \vartheta(p),$ and $\varphi(p)$. If the path p is that of an observer drifting with the ether, parametrized by his proper time, then Eq. (12) must agree with Eq. (10). Therefore $\dot{\vartheta} = \dot{\varphi} = 0$, meaning that the drift is radial. Further, $\dot{t} = 1$, which says that coordinate time elapses at the same rate as the proper time of the drifting observer. Finally, $\dot{\rho} = f(\rho)$, and it then follows that the coordinate 3-velocity of the drifting ether is $f(\rho)\partial/\partial\rho$, and that the coordinate 3-speed is $|f(\rho)|$.

For the discussion of horizons in Sec. V it will be required that a little about the paths of light rays be known. If p is any null path, then from Eq. (12) it follows that

$$\left(\frac{d\rho}{dt} - f(\rho)\right)^2 + r^2(\rho)\left(\frac{d\Omega}{dt}\right)^2 = 1, \tag{13}$$

unless $\dot{t} = 0$, in which case also $\dot{\rho} = \dot{\vartheta} = \dot{\varphi} = 0$ and p is not a path of a light ray. Inasmuch as the relative coordinate 3-velocity of the path p with respect to the ether flow is

$$\left(\frac{d\rho}{dt} - f(\rho)\right)\frac{\partial}{\partial\rho}(p) + \frac{d\vartheta}{dt}\frac{\partial}{\partial\vartheta}(p) + \frac{d\varphi}{dt}\frac{\partial}{\partial\varphi}(p), \tag{14}$$

the import of Eq. (13) is that the square of the speed of light with respect to the ether, as measured in the coordinate system $[t, \rho, \vartheta, \varphi]$, is 1.

Each of the vector fields $u \pm \partial/\partial\rho$ generates a congruence of null geodesics, for if

$$\dot{p} = u(p) \pm \frac{\partial}{\partial\rho}(p)$$
$$= e_0(p) \pm e_1(p), \tag{15}$$

then $\dot{p}$ is null, and, in view of Eq. (7),

$$\ddot{p} = de_0(p)\dot{p} \pm de_1(p)\dot{p}$$
$$= (de_0 e_0 \pm de_0 e_1 \pm de_1 e_0 + de_1 e_1)(p) \tag{16}$$
$$= f'\dot{p}.$$

The coordinate 3-velocities of the null geodesics in these two congruences, and their coordinate 3-velocities with respect to the ether flow, are, respectively,

$$[f(\rho) \pm 1]\,\partial/\partial\rho \quad \text{and} \quad \pm\,\partial/\partial\rho. \tag{17}$$

Light rays following these paths are moving in the radial direction if they are moving at all. Those in one group move upstream in the ether, and those in the other group go downstream.

IV. THE CURVATURE TENSOR FIELDS

It is a simple matter to calculate the curvature forms $\Theta_\kappa{}^\mu$ from the formulas (7) for the connection forms $\omega_\kappa{}^\mu$. The result is that

$$
[\Theta_\kappa{}^\mu] =
\begin{bmatrix}
\left(\dfrac{f^2}{2}\right)''(\omega^0 \wedge \omega^1) & 0 & - & - \\[2ex]
\dfrac{(r'f)'f}{r}(\omega^0 \wedge \omega^2) + \dfrac{r''}{r}f(\omega^1 \wedge \omega^2) & -\dfrac{r''}{r}f(\omega^0 \wedge \omega^2) + \left[\dfrac{r'}{r}\left(\dfrac{f^2}{2}\right)' - \dfrac{r''}{r}\right](\omega^1 \wedge \omega^2) & 0 & - \\[3ex]
\dfrac{(r'f)'f}{r}(\omega^0 \wedge \omega^3) + \dfrac{r''}{r}f(\omega^1 \wedge \omega^3) & -\dfrac{r''}{r}f(\omega^0 \wedge \omega^3) + \left[\dfrac{r'}{r}\left(\dfrac{f^2}{2}\right)' - \dfrac{r''}{r}\right](\omega^1 \wedge \omega^3) & \dfrac{1 - (1 - f^2)r'^2}{r^2}(\omega^2 \wedge \omega^3) & 0
\end{bmatrix} .
\tag{18}
$$

The isolated + and − signs are meant to reflect the symmetry $\Theta_0{}^m = \Theta_m{}^0$ and the antisymmetry $\Theta_k{}^m = -\Theta_m{}^k$ for $k, m = 1, 2, 3$.

A brief additional calculation finds the nonvanishing components of the Ricci curvature tensor field to be given by

$$
R_{00} = \nabla^2(\tfrac{1}{2}f^2) + 2(r''/r)f^2,
$$
$$
R_{01} = R_{10} = 2(r''/r)f,
$$
$$
R_{11} = -\nabla^2(\tfrac{1}{2}f^2) + 2r''/r, \tag{19}
$$
$$
R_{22} = R_{33} = \{[(\tfrac{1}{2}r^2)'(1 - f^2)]' - 1\}/r^2.
$$

Here ∇^2 is the Laplacian for any one of the spacelike hypersurfaces Σ_t orthogonal to u; it is determined by the Riemannian line element (3). For a function $h(\rho)$,

$$
\nabla^2[h(\rho)] = [1/r^2(\rho)](r^2h')'(\rho). \tag{20}
$$

The scalar field $f^2/2$ that appears in these formulas is $\tfrac{1}{2}(1 - g_{00})$, as calculated in the coordinate system $[t, \rho, \vartheta, \varphi]$. As such, it is the conventional general-relativistic analog, for the gravitational field described by the line element (1), of the negative of the Newtonian gravitational potential. By the same token $-\nabla(f^2/2)$ is the analog of Newton's force of gravity. If the ether flow rate $|f|$ is constant, then this gradient is 0, and, following convention, one has to say that in this case the gravitational field exerts on test particles no force in the Newtonian sense. It is this observation which provides the rationale to identify "gravity" with the internal, relative motions of the postulated ether, as distinguished from its overall rigid motions.

V. HORIZONS

The line element (1) assumes a familiar form upon introduction of a new coordinate T satisfying

$$
dT = dt + f(\rho)[1 - f^2(\rho)]^{-1}d\rho. \tag{21}
$$

It is

$$
d\tau^2 = [1 - f^2(\rho)]dT^2 - [1 - f^2(\rho)]^{-1}d\rho^2
$$
$$
- r^2(\rho)d\Omega^2. \tag{1_S}
$$

This is analogous to the usual orthogonal form of Schwarzschild's vacuum line element and reduces to it when $r(\rho) = \rho$ and $f^2(\rho) = 2m/\rho$, m being the mass parameter. It is clear from Eq. (1_S) that the translations along the T coordinate curves are isometries, hence that $\partial/\partial T$ is a Killing vector field. It is also clear that $\partial/\partial T$ is everywhere orthogonal to the hypersurfaces on which T is constant. Therefore, wherever $f^2 < 1$, so that $\partial/\partial T$ is timelike, the manifold is static. This was stated in Sec. II to be the case; it was also said at that point that $\partial/\partial t$ is hypersurface orthogonal, and this now follows from the determination that $\partial/\partial t = \partial/\partial T$.

The Schwarzschild horizon, where $\rho = 2m$, corresponds in the general case to 2-spheres $S_{t,\rho}$ on which $f(\rho) = \pm 1$. The ether-flow picture includes a graphic interpretation of such horizons. On each such sphere the coordinate speed of the drifting ether, which is $|f(\rho)|$, just matches the speed of light with respect to the ether. From Eq. (13) it follows that if $S_{t,\rho}$ is intersected by the null path p, then $0 \le d\rho/dt \le 2$ if $f(\rho) = 1$, but $-2 \le d\rho/dt \le 0$ if $f(\rho) = -1$; therefore, if p crosses $S_{t,\rho}$, its radial velocity component and that of the ether flow cannot be oppositely directed at the crossing point. Thus light rays can only cross a horizon in the downstream direction of the flow. One can easily check that the only paths of light rays that contact a horizon without crossing it belong to the upstream member of the pair of radial null congruences mentioned in Sec. III; these light rays remain forever on the horizon, struggling to go nowhere. In regions where $f^2(\rho) > 1$, such as Schwarzschild interiors, all light rays are swept along downstream, even those whose motion relative to the ether is upstream. In regions where $f^2(\rho) < 1$, such as Schwarzschild exteriors, some are able to progress upstream, but only with difficulty when near the horizon. People in light canoes should avoid ethereal rapids!

Another space–time manifold whose line element can assume the forms (1) and (1_S), and that possesses a horizon, is the de Sitter cosmological model,[11,12] for which $r(\rho) = \rho$ and $f^2(\rho) = (\rho/R)^2$, R being a positive parameter. It models a universe that is devoid of mat-

ter yet exhibits gravitational effects. Test particles in this universe cannot remain at rest with respect to one another, for they have to share in a cosmological expansion or contraction, which may be identified with a linear expansion or contraction of the ether, reflected in the form that f has. The 2-spheres $S_{t,R}$ constitute a horizon which is the edge of the field of vision for all observers on the upstream side of it. Here, again, gravity corresponds to nonrigid motions of the ether.

VI. THE SCALAR FIELD AS PLUMBER'S FRIEND

We come now to the task of opening up the Schwarzschild singularity so that the ether may flow through unimpededly. To discover the cause of the constriction, let us refer to the formulas (19) for the components of the Ricci curvature tensor field and observe that the Einstein vacuum field equations $R_{00} = R_{01} = R_{11} = 0$ imply that $r'' = 0$, hence that $r(\rho)$ is a linear function of ρ, which in view of the field equation $R_{22} = 0$ cannot be constant, that r must therefore have a zero, and that as ρ approaches this zero the 2-spheres $S_{t,\rho}$ shrink to points, these points constituting the Schwarzschild singularity. In this way we may identify as the cause of constriction an excess of strength in the Einstein vacuum field equations. To weaken these equations and thereby to remove the constriction, an aid is required, a plumber's friend so to speak. Let us find one.

The Ricci tensor field is $\omega^\kappa \otimes R_{\kappa\lambda}\omega^\lambda$, where the $R_{\kappa\lambda}$ are given by Eqs. (19). Look at the terms that involve r''. Their sum can be factored:

$$2(r''/r)[f^2(\omega^0 \otimes \omega^0) + f(\omega^0 \otimes \omega^1 + \omega^1 \otimes \omega^0) + \omega^1 \otimes \omega^1]$$

$$= 2(r''/r)(f\omega^0 + \omega^1) \otimes (f\omega^0 + \omega^1) \qquad (22)$$

$$= 2(r''/r)(d\rho \otimes d\rho).$$

Now let α be a nonconstant, differentiable, real-valued function on the real line, and let $\phi = \alpha(\rho)$. Then the square of the gradient of the scalar field ϕ is given by

$$d\phi \otimes d\phi = \alpha'^2(d\rho \otimes d\rho). \qquad (23)$$

Upon comparing Eq. (23) with Eq. (22) we see that a field equation of the form

$$\text{Ricci tensor field} = K(d\phi \otimes d\phi), \qquad (24)$$

with nonzero coupling constant K, will replace the unwanted condition $r'' = 0$ with the less restrictive condition $r'' = \frac{1}{2}K\alpha'^2 r$. This latter condition implies that the radius function r is convex if $K > 0$, but concave if $K < 0$. If r is concave, then it is impossible for the space-time manifold $\mathfrak{M}$ to have a central hole such as the one that Fig. 1 shows a cross section of. The reason is that on each great-circle cross section of a typical spatial cross section Σ_t of $\mathfrak{M}$ the induced Gaussian curvature is given by the scalar field $-r''/r$. Concavity of r renders this curvature everywhere nonnegative, which in a hole of the kind envisioned it cannot be. To enlarge the Schwarzschild singularity into a proper hole, we must therefore take $K > 0$ so that r will be convex.[13]

As it happens, the coupling expressed by Eq. (24) is known to derive from the simple variational principle

$$0 = \delta \int (-g)^{1/2} (R^\kappa{}_\kappa - K\phi^{\cdot\kappa}\phi_{,\kappa})d^4x. \qquad (25)$$

Once K has been made positive in Eq. (25), it may be replaced by the number 2, for this involves at most a rescaling of ϕ. Then the Euler equations that together are equivalent to the variational principle are

$$R_{\mu\nu} - \frac{1}{2}R^\kappa{}_\kappa g_{\mu\nu} = 2(\phi_{,\mu}\phi_{,\nu} - \frac{1}{2}\phi^{\cdot\kappa}\phi_{,\kappa}g_{\mu\nu}) \qquad (26)$$

and the scalar wave equation

$$\Box\phi \cong \text{Tr } \mathbf{d}(G^{-1}d\phi) = \phi^{\cdot\kappa}{}_{;\kappa} = 0, \qquad (27)$$

in which G is the metric tensor field. Equation (26) is equivalent to

$$R_{\mu\nu} = 2\phi_{,\mu}\phi_{,\nu}, \qquad (28)$$

which in turn is equivalent to Eq. (24) with $K = 2$.

These are the field equations by way of which the scalar field ϕ will be applied to the ethereal plumbing problem. The next section will present all of their solution manifolds that have line elements of the form in Eq. (1), as well as the analogous solutions for the equations that would have resulted had K been taken negative. Of the former, one will turn out to be geodesically complete (also static and possessed of a central hole); of the latter, none will.

VII. THE ETHER-FLOW, DRAINHOLE, PARTICLE MODEL

Under the assumption that $\phi = \alpha(\rho)$, the wave equation (27) is equivalent to

$$[r^2(f^2 - 1)\alpha']' = 0, \qquad (29)$$

and the field equations (28) are equivalent to the three equations

$$r''/r = \alpha'^2, \qquad (30)$$

$$[r^2(f^2/2)']' = 0, \qquad (31)$$

$$[(r^2/2)'(1 - f^2)]' = 1. \qquad (32)$$

The last two yield, upon integration and rearrangement,

$$r^2(1 - f^2)' = 2m \qquad (33)$$

and

$$r^{2'}(1 - f^2) = 2(\rho - m), \qquad (34)$$

where without loss of generality the zero point of ρ has been adjusted to equalize the integration constants. Combined, these equations produce, after integration,

$$r^2(1 - f^2) = \rho^2 + C. \qquad (35)$$

Also, Eq. (29) integrates to

$$\alpha' = -n/[r^2(1 - f^2)] = -n/(\rho^2 + C). \qquad (36)$$

From Eqs. (34) and (35) it follows that

$$r'/r = (\rho - m)/(\rho^2 + C), \qquad (37)$$

hence that

$$r''/r = (r'/r)' + (r'/r)^2 = (C + m^2)/(\rho^2 + C)^2. \qquad (38)$$

Thus Eq. (30) adds only the information that $C = n^2 - m^2$. Equations (36) and (37) now imply that

$$r^2(\rho) = |\rho^2 + n^2 - m^2| \, e^{(2m/n)\alpha(\rho)}, \qquad (39)$$

provided α is made to absorb additively the integration constant, which it can do with no change in α', hence with no effect on the field equations.

At this stage Eq. (1_S) for the line element has been specialized to

$$d\tau^2 = \text{sgn}(\rho^2 + n^2 - m^2)\{ e^{-(2m/n)\alpha(\rho)} dT^2$$
$$- e^{(2m/n)\alpha(\rho)}[d\rho^2 + (\rho^2 + n^2 - m^2)d\Omega^2]\}, \qquad (1_{S,\alpha})$$

and the only integration left to be done is that of Eq. (36), which now reads

$$\alpha' = -n/(\rho^2 + n^2 - m^2). \qquad (36')$$

This requires consideration of three cases: (I) $n^2 < m^2$; (II) $n^2 = m^2$; (III) $n^2 > m^2$. In each case n will be taken to be nonnegative, for at the end only n^2 will appear. Also, the boundary condition that

$$\lim_{\rho \to \infty} \phi \equiv \lim_{\rho \to \infty} \alpha(\rho) = 0 \qquad (40)$$

will be applied. This limit always exists; requiring it to be 0 is equivalent to requiring that the line element in the form $(1_{S,\alpha})$ be asymptotic to a Schwarzschild vacuum line element (with mass parameter m, it turns out). Within isometric equivalence this boundary condition does not reduce the set of solution manifolds, the reason being that it has no effect on α', and only α' appears in the field equations.

Case I $(n^2 < m^2)$

Let $a = (m^2 - n^2)^{1/2}$. Then

$$\alpha'(\rho) = -n/(\rho^2 - a^2),$$

$$\alpha(\rho) = (n/2a)\log|(\rho + a)/(\rho - a)|,$$

$$r^2(\rho) = |\rho^2 - a^2| \cdot |(\rho + a)/(\rho - a)|^{m/a} \qquad (41)$$

$$= |\rho + a|^{(m/a)+1}/|\rho - a|^{(m/a)-1},$$

$$f^2(\rho) = 1 - \text{sgn}(\rho^2 - a^2)|(\rho - a)/(\rho + a)|^{m/a}.$$

When $n > 0$, there is a separation of the space–time manifold $\mathfrak{M}$ to which these formulas apply into three connected submanifolds, corresponding to the radial coordinate ranges $\rho < -a$, $-a < \rho < a$, and $a < \rho$. If $m \neq 0$, the formula for $f^2(\rho)$ implies that $f^2 > 0$ on two of these submanifolds, but that $f^2 < 0$ on the other one, namely, the one corresponding to $\rho < -a$, if $m > 0$, but the one corresponding to $a < \rho$, if $m < 0$. Because f is imaginary, the line element on this submanifold, though real in the form (1_S), is complex in the form (1), and t must be interpreted as a complex coordinate, related to the real coordinates T and ρ by Eq. (21). The computations that have gone before all remain valid, but the description of the geometry and the interpretation of the vector field u must be modified. In particular the cross sections Σ_t are two-dimensional instead of three-dimensional, and u is complex instead of real. There is no horizon of the Schwarzschild type on this submanifold, for these occur only where $f^2(\rho) = 1$.

In the two submanifolds of $\mathfrak{M}$ on which $f^2 > 0$ the typical spatial cross section Σ_t is three-dimensional, and its shape is determined by the function r, whose graph

when $m > 0$ is shown in Fig. 2. (Reflection of this graph through the vertical axis produces the graph of r when $m < 0$.) If, let us say, $m > 0$, then in the submanifold on which $a < \rho$ the radius $r(\rho)$ of the 2-sphere $S_{t,\rho}$ decreases from ∞ to a positive minimum value $r(m)$ as ρ decreases from ∞ to m, after which it returns to ∞ as $\rho \to a$. Therefore, each cross section Σ_t in this submanifold has a central hole of positive minimum radius $r(m)$. In the other submanifold, $S_{t,\rho}$ undergoes infinite expansion as $\rho \to a$, but shrinks toward point size as $\rho \to -a$; the cross section Σ_t thus has in its center only a pinhole and not a hole of positive radius. Neither of these two submanifolds has a horizon except in the asymptotic sense that $f^2(\rho) \to 1$ as $\rho \to a$. When $m < 0$, their geometry is demonstrably the same.

The Schwarzschild manifold occurs when $n = 0$, in which case $a = |m|$ and m is the Schwarzschild mass. The graph of r when $m > 0$ is included in Fig. 2. The Schwarzschild singularity, where $r(\rho) = 0$, corresponds to $\rho = -m$, and the horizon, where $f^2(\rho) = 1$, to $\rho = m$.

An illumination is cast upon the Schwarzschild solution by the observation that it is unstable as a solution of the field equations (26) and (27) in that, as $n \to 0$, r converges pointwise to the Schwarzschild form, but not uniformly. The two submanifolds on which $f^2 > 0$ coalesce, but only reluctantly, at the Schwarzschild horizon. This phenomenon is another aspect of the behavior of the Schwarzschild horizon under perturbations, discussed by Janis, Newman, and Winicour,[14] and by Penney.[15] They have found and examined a solution of the field equations used here, but with the coupling constant negative rather than positive—for them $K < 0$ in the variational principle (25). Their line element is the same, but for choice of coordinate system and parameter names, as the one given by Eqs. (41)
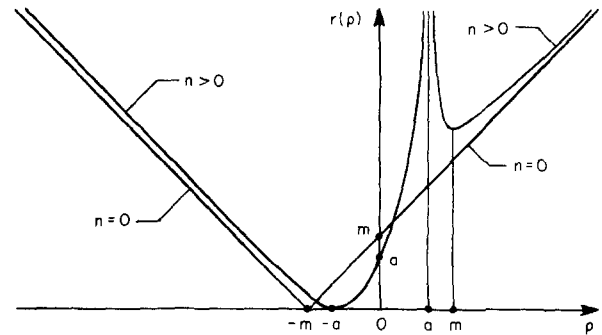

FIG. 2. The graph, for $m > 0$, of the radius function r in Case I $(n^2 < m^2)$. Here $r^2(\rho) = |\rho + a|^{1+m/a}|\rho - a|^{1-m/a}$, and $a = (m^2 - n^2)^{1/2}$. For $m < 0$, reflect the graph through the vertical axis.
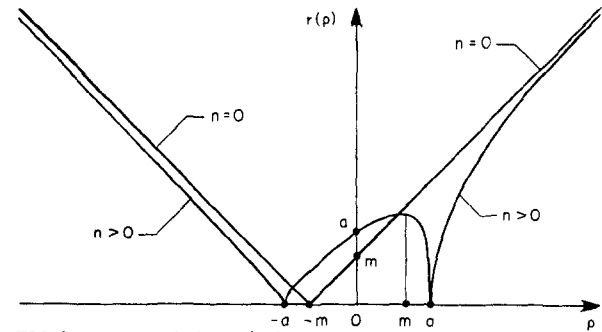

FIG. 3. The graph, for $m > 0$, of the radius function r obtained from the Case I solution by replacing n^2 with $-n^2$. Here $r^2(\rho) = |\rho + a|^{1+m/a} \times |\rho - a|^{1-m/a}$, and $a = (m^2 + n^2)^{1/2}$. The corresponding line element satisfies the field equations generated by the variational principal of Eq. (26) with $K = -2$.

with $a = (m^2 + n^2)^{1/2}$. As such, it is the only solution of the negatively coupled field equations that can take the form of Eq. (1), except the solution, falling under Case II, in which $m = n = 0$. The graph of the radius function r for this solution is depicted in Fig. 3, again under the assumption that $m > 0$. This r likewise converges pointwise but not uniformly to the Schwarzschild r as $n \to 0$. And here, also, there is, when $n > 0$, separation of $\mathfrak{M}$ at $-a$ and a into three connected submanifolds, none containing a horizon. As was forecast in Sec. VI, r is concave; hence none of these submanifolds has more than a pinhole at its center. This solution was earlier discovered by Bergmann and Leipnik.[16]

Using Eq. (18), and assuming either coupling polarity, one can easily see that if $n > 0$, then at each of the edges where $\rho^2 \to a^2$ some of the curvature components become infinite, but that if $n = 0$, this happens only at the edges where $\rho \to -m$. Because the frame system $\{e_\mu\}$ is orthonormal, these apparent singularities in curvature are real. Owing to their presence, it is impossible to extend metrically across one of these edges any submanifold of $\mathfrak{M}$. For this reason neither $\mathfrak{M}$ nor any possible metric extension of $\mathfrak{M}$ will be geodesically complete if there is a geodesic in $\mathfrak{M}$ that arrives at one of these edges without using up its affine parameter. That there are such geodesics will be established in Sec. VIII.

Case II $(n^2 = m^2)$

Here

$$\alpha'(\rho) = -n/\rho^2, \quad \alpha(\rho) = n/\rho$$
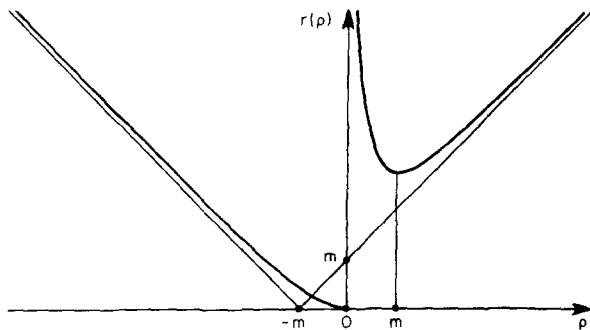$$r^2(\rho) = \rho^2 e^{2m/\rho}, \quad f^2(\rho) = 1 - e^{-2m/\rho}. \tag{42}$$

FIG. 4. The graph, for $m > 0$, of the radius function r in Case II $(n^2 = m^2)$. Here $r^2(\rho) = \rho^2 e^{2m/\rho}$. For $m < 0$, reflect the graph through the vertical axis.
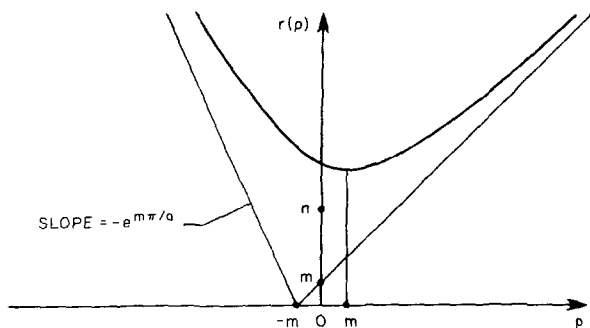
FIG. 5. The graph for $m \geq 0$, of the radius function r in Case III $(n^2 > m^2)$. Here $r^2(\rho) = (\rho^2 + a^2) e^{(2m/n)\alpha(\rho)}$, $\alpha(\rho) = (n/a)[\pi/2 - \tan^{-1}(\rho/a)]$, and $a = (n^2 - m^2)^{1/2}$. The minimum value of r, namely $r(m)$, is the radius of the drainhole; it ranges from n up to $ne-$ as m goes from 0 to $n-$, and it always exceeds $2m$. That the associated manifold $\mathfrak{M}_{m,n}$ is asymptotically Schwarzschildean as $\rho \to \infty$ is reflected in the relation $r(\rho) \sim \rho + m$ as $\rho \to \infty$.

This is the limiting case of Case I as $a \to 0$. The manifold on which $-a < \rho < a$ has been squeezed out. The two remaining manifolds, corresponding now to $\rho < 0$ and $0 < \rho$, are in all qualitative aspects, including infinite edge curvatures, unchanged (unless $m = n = 0$, which results in two copies of flat Minkowski spacetime). In particular, if $m \neq 0$, neither of them possesses a horizon, is metrically extendible, or is geodesically complete. The graph of r for $m > 0$ is shown in Fig. 4. The line element has been exhibited by Yilmaz in the form $(1_{S,\alpha})$.[17]

Case III $(n^2 > m^2)$

This is the case of greatest interest, for the line element measures a connected and geodesically complete space-time manifold with a drainhole. Let $a = (n^2 - m^2)^{1/2}$. Then

$$\alpha'(\rho) = -n/(\rho^2 + a^2), \quad \alpha(\rho) = (n/a)[\tfrac{1}{2}\pi - \tan^{-1}(\rho/a)],$$
$$r^2(\rho) = (\rho^2 + a^2) e^{(2m/n)\alpha(\rho)}, \quad f^2(\rho) = 1 - e^{-(2m/n)\alpha(\rho)}. \tag{43}$$

Because r^2 and $1 - f^2$ are everywhere analytic and positive, these formulas determine an analytic line element of the form (1_S), which now becomes $(1_{S,\alpha})$ with $n^2 - m^2 = a^2$. This line element fits a manifold on which the coordinate ρ ranges from $-\infty$ to ∞, as does also the coordinate T. This manifold will be shown in the next section to be geodesically complete. Let it be denoted $\mathfrak{M}_{m,n}$.

If $m \geq 0$, then $0 \leq f^2 < 1$, and the form (1) of the line element of $\mathfrak{M}_{m,n}$ is real. The relation between the time coordinates t and T, expressed by Eq. (21), depends upon whether $f \geq 0$ or $f \leq 0$, but in either event t is real and ranges from $-\infty$ to ∞. If $m = 0$, then $f = 0$ (the ether is at rest). When $m > 0$, $f^2(\rho)$ decreases from $1 - e^{-2m\pi/a}$ to 0 as ρ goes from $-\infty$ to ∞. There is no horizon, because $f^2(\rho)$ is never 1.

Figure 5 displays the graph of the radius function r when $m \geq 0$. The 2-spheres $S_{t,\rho}$ of constant t and constant ρ are smallest when $\rho = m$; they undergo infinite expansion both as $\rho \to \infty$ and as $\rho \to -\infty$. It follows from Eqs. (43) that the minimum radius $r(m)$, considered as a function of m, increases from n to $ne-$ as m goes from 0 to $n-$. Thus the order of magnitude of the radius of the drainhole is determined by n, the only noticeable effect of m being to bound it below via the first two of the inequalities $m < n \leq r(m) < ne$ (actually, as Fig. 5 shows, $r(m) > 2m$).

It is not difficult to establish that the following asymptotic relations hold, whether $m > 0$, $m = 0$, or $m < 0$: as $\rho \to \infty$,

$$\alpha(\rho) = (n/\rho) + O(1/\rho^3),$$
$$r(\rho) = (\rho + m) + O(1/\rho), \tag{44}$$
$$f^2(\rho) = [2m/(\rho + m)] + O(1/\rho^2);$$

as $\rho \to -\infty$,

$$\alpha(\rho) = (n\pi/a) + (n/\rho) + O(1/\rho^3),$$
$$r(\rho) = -(\rho + m) e^{m\pi/a} + O(1/\rho), \tag{45}$$
$$f^2(\rho) = 1 - e^{-2m\pi/a}[1 - 2m/(\rho + m)] + O(1/\rho^2).$$

These relations imply that the manifold $\mathfrak{M}_{m,n}$ is, in the

usual loose sense, asymptotic as $\rho \to \infty$ to the Schwarzschild manifold with mass parameter m. They also imply that $\mathfrak{M}_{m,n}$ is asymptotically flat, both as $\rho \to \infty$ and as $\rho \to -\infty$, because, as may easily be checked, the coefficients $(f^2/2)''$, $(r'f)'f/r$, etc., in the expression (18) for the curvature forms $\Theta_\kappa{}^\mu$ are asymptotic to 0. (This criterion for asymptotic flatness is acceptable because the frame system $\{e_\mu\}$ is orthonormal.) It is natural to ask if $\mathfrak{M}_{m,n}$ is also asymptotically Schwarzschildean as $\rho \to -\infty$. The answer is that $\mathfrak{M}_{m,n}$ is asymptotic as $\rho \to -\infty$ to the Schwarzschild manifold with mass parameter $-me^{m\pi/a}$. This somewhat surprising conclusion is a consequence of the observation that if $\bar{m} = -me^{m\pi/a}$ and $\bar{n} = ne^{m\pi/a}$, then there is an isometry between $\mathfrak{M}_{m,n}$ and $\mathfrak{M}_{\bar{m},\bar{n}}$ which reverses the direction of increase of the radial coordinate and thus matches up opposed asymptotic regions. Such an isometry is obtained by identifying the point of $\mathfrak{M}_{m,n}$ having S-type coordinates $[T, \rho, \vartheta, \varphi]$ with the point of $\mathfrak{M}_{\bar{m},\bar{n}}$ whose S-type coordinates are $[Te^{-m\pi/a}, -\rho e^{m\pi/a}, \vartheta, \varphi]$.

Because these isometries exist, no physically useful distinction can be drawn between the manifolds with positive mass parameters m and those for which m is negative. On the other hand, in each such manifold there is a clear physical distinction between the two sides of the drainhole, for one side is asymptotic to a Schwarzschild manifold whose mass parameter is positive, while the other is asymptotic to a Schwarzschild manifold whose mass parameter is negative. In the study of the geodesics of $\mathfrak{M}_{m,n}$ it will appear that, when $m > 0$, test particles are always accelerated in the direction of decreasing ρ. This is toward the drainhole when $\rho > m$, but away from it when $\rho < m$. Thus if $m > 0$ (and likewise if $m < 0$), the manifold $\mathfrak{M}_{m,n}$ models a Janus-faced particle that attracts matter on one side and repels it (more strongly) on the other.

The curious asymmetry between the positive mass, say m, and the negative mass $\bar{m}$ of the particle, expressed by the equation

$$\bar{m}/m = -\exp[m\pi/(n^2 - m^2)^{1/2}], \qquad (46)$$

is a facet of the model that is especially eye-catching. It is even more so in light of the observation that certain not unnatural specifications of m and n will cause the equation to generate some of Dirac's outsized, dimensionless physical "constants", which are about 10^{20k}, where k is some small nonzero integer.[18] Specifically, if m is of the order of a proton mass, 1.2×10^{-52} cm, while n is of the order of Planck's length, 1.6×10^{-33} cm, then $-\bar{m}/m \approx 1 + 10^{-19}$. If instead $n \approx 2.8 \times 10^{-13}$ cm, the classical electron radius, then $-\bar{m}/m \approx 1 + 10^{-39}$. A speculative extrapolation from the asymmetry between m and $\bar{m}$ is that the universe expands because it contains more negative mass than positive, each half-particle of positive mass m being slightly overbalanced by a half-particle of negative mass $\bar{m}$ such that $-\bar{m} > m$.

The case where $m = 0$ is particularly interesting. The ether is not flowing, because $f = 0$. However, the drainhole remains open, because $r(\rho) = (\rho^2 + n^2)^{1/2} \geq n > 0$. The manifold is symmetric with respect to reflection through the drainhole. The catenoid of Fig. 1 is the cross section of $\mathfrak{M}_{0,n}$ on which $t = 0$ and $\vartheta = \pi/2$. Although massless, the particle modeled interacts with test particles, as the study of its geodesics will show.

The scalar field ϕ that holds the drainhole open satisfies the scalar wave equation. If in the flowless case some disturbance were to cause the drainhole to pinch in two, there would be left on each side a central bump in a topologically and asymptotically Euclidean 3-space. These bumps, being directly associated with ϕ via the field equations (28), would radiate away with the fundamental speed of wave propagation. The particle would have dematerialized from a drainhole to a ϕ-wave. When $m \neq 0$, the same thing presumably could happen, but in addition there should arise a traveling gradient in the ether flow, identifiable, one imagines, as gravitational radiation. Such a picture of changing topology and geometry provides a graspable basis for attempts at understanding the wave-particle duality of matter.

VIII. GEODESICS AROUND, ABOUT, AND THROUGH THE DRAINHOLE

The starting point for the study of the geodesics of the manifold $\mathfrak{M}$ bearing the line element (1) is the earlier equation

$$\dot{p} = \dot{t}e_0(p) + [\dot{\rho} - f(\rho)\dot{t}]e_1(p) + r(\rho)\dot{\vartheta}e_2(p) + r(\rho)(\sin\vartheta)\dot{\varphi}e_3(p), \qquad (12)$$

which holds for every path p in $\mathfrak{M}$. From Eqs. (12), (A3), (A1), (7), and (5) it follows that

$$\ddot{p} = \left[\ddot{t} + f'(\dot{\rho} - f\dot{t})^2 + f\left(\frac{r^2}{2}\right)' \dot{\Omega}^2\right]\frac{\partial}{\partial t}(p)$$
$$+ \left[\ddot{\rho} - \left(\frac{f^2}{2}\right)'[\dot{t}^2 - (\dot{\rho} - f\dot{t})^2]\right.$$
$$\left. - (1 - f^2)\left(\frac{r^2}{2}\right)'\dot{\Omega}^2\right]\frac{\partial}{\partial\rho}(p)$$
$$+ \left[\ddot{\vartheta} + 2\frac{r'}{r}\dot{\rho}\dot{\vartheta} - (\sin\vartheta)(\cos\vartheta)\dot{\varphi}^2\right]\frac{\partial}{\partial\vartheta}(p)$$
$$+ \left(\ddot{\varphi} + 2\frac{r'}{r}\dot{\rho}\dot{\varphi} + 2(\text{ctn}\vartheta)\dot{\vartheta}\dot{\varphi}\right)\frac{\partial}{\partial\varphi}(p), \qquad (47)$$

where

$$\dot{\Omega}^2 = \dot{\vartheta}^2 + (\sin\vartheta)^2\dot{\varphi}^2. \qquad (48)$$

Now let p be a maximally extended geodesic path, affinely parametrized, so that $\ddot{p} = 0$. This equation is equivalent to the four scalar equations that say that the components of $\ddot{p}$ in Eq. (47) are 0. For reference call these the t-, ρ-, ϑ-, and φ-equations.

Reflecting the spherical symmetry of the metric, the ϑ- and φ-equations entail that the orbit of the path p lies in one of the great-circle cross sections of $\mathfrak{M}$, which are those hyperspaces typified by the equatorial cross section, defined by $\vartheta = \pi/2$. The angular-momentum first integral of the ϑ- and φ-equations is

$$r^2\dot{\Omega} = h. \qquad (49)$$

The t- and ρ-equations have the first integral

$$(1 - f^2)\dot{t} + f\dot{\rho} = k. \qquad (50)$$

Suppose next that the parameter on p is the proper time along p if p is timelike, the proper distance along p if p is spacelike. Then the t-, ρ-, ϑ-, and φ-equations have the first integral

$$\epsilon = |\dot{p}|^2 = \dot{t}^2 - (\dot{\rho} - f\dot{t})^2 - r^2\dot{\Omega}^2, \qquad (51)$$

where ϵ, the indicator of p, is 1, 0, or -1, according as p is timelike, null, or spacelike. A consequence of Eqs. (49), (50), and (51) is that

$$\dot{\rho}^2 = k^2 - (1 - f^2)(\epsilon + h^2/r^2). \tag{52}$$

When the first integral (51) is used in the ρ-equation, there results

$$\ddot{\rho} = \epsilon(\tfrac{1}{2}f^2)' + \tfrac{1}{2}[(r^2)'(1 - f^2) - (r^2)(1 - f^2)']\dot{\Omega}^2. \tag{53}$$

If we utilize the integrals (33) and (34) of the field equations, then Eq. (53) becomes

$$\ddot{\rho} = \epsilon(-m/r^2) + (\rho - 2m)\dot{\Omega}^2. \tag{54}$$

This equation applies in each of Cases I, II, and III of Sec. VII. It implies that, when $m > 0$, test particles on radial paths are always accelerated in the direction of decreasing ρ. In Case III this means that the drainhole attracts matter on the side identified by asymptotic comparison to a Schwarzschild manifold as having positive mass, and repels it on the side to which negative mass has been ascribed.

Completeness

For a null, radial geodesic, $\epsilon = h = 0$, and Eq. (52) implies that $\dot{\rho} = \pm k$. If $k = 0$, then ρ is constant, and Eq. (50) allows two possibilities. One is that $\dot{t} = 0$, in which case t, also, is constant; the geodesic is degenerate, frozen at one point of space–time. The other possibility is that $f^2(\rho) = 1$; in this case the light signal whose path is p is stuck on a horizon, but not frozen in time. If on the other hand $k \neq 0$, then ρ is a nonconstant, linear function of the affine parameter. From this it follows that if $\mathfrak{M}$ is any one of the nonflat space–time manifolds discussed under Cases I and II of Sec. VII, then $\mathfrak{M}$ has null radial geodesics that come up to an edge where there are infinite curvatures without exhausting their affine parameters in the process. As was remarked in Sec. VII, this implies that none of those manifolds has a geodesically complete extension.

Turning now to Case III, let us see whether the space–time manifold $\mathfrak{M}_{m,n}$ is geodesically complete. Denote by p^+ that portion of the path p on which the parameter is nonnegative. If p^+ is confined to a compact region of the manifold, then p^+ includes all nonnegative numbers in its parameter interval, for p is by hypothesis maximally extended. If p^+ is not so confined, then either $\rho(p^+)$ or $t(p^+)$ is unbounded. But $f^2(\rho)$ and $r^2(\rho)$ are defined for all values of ρ, and both $1 - f^2$ and $1/r^2$ are bounded. Hence Eq. (52) implies that $\dot{\rho}$ is bounded. On the other hand, $1/(1 - f^2)$ is bounded, and, therefore, in view of Eq. (50), $\dot{t}$ is bounded. No unbounded function with bounded derivative is restricted to a bounded interval, so that again the parameter of p consumes all the nonnegative numbers. In the same fashion p's parameter uses up all the nonpositive numbers. Therefore, $\mathfrak{M}_{m,n}$ is indeed geodesically complete.

It is interesting to note that completeness depends only upon these properties of f^2 and r^2 in addition to the smoothness that they possess: (a) Each of f^2 and r^2 is defined on the interval $(-\infty, \infty)$; (b) r^2 is bounded away from 0, so that there is in fact a hole in the manifold that is bigger than a point; (c) f^2 is bounded; (d) f^2 is bounded away from 1, which means that there is no

horizon, not even an asymptotic one at an edge of the manifold.

Goedesics of $\mathfrak{M}_{0,n}$

In describing the geodesics of the manifolds $\mathfrak{M}_{m,n}$ of Case III it will be easiest to treat $\mathfrak{M}_{0,n}$ separately. The condition $m = 0$ is equivalent to $f = 0$; the first part of the discussion will apply merely if $f = 0$, irrespective of whether any field equations are satisfied. The line element (1) decomposes into a purely temporal part and a purely spatial part; this shows up in Eq. (51), which now reads

$$\epsilon = \dot{t}^2 - \dot{\sigma}^2, \tag{55}$$

where

$$\dot{\sigma}^2 = \dot{\rho}^2 + r^2(\rho)\dot{\Omega}^2. \tag{56}$$

Because of this decomposition the Killing vector field $\partial/\partial t$ is orthogonal to the spatial cross sections Σ_t, and the projection of the geodesic path p on any one Σ_t via translation of its points along the t lines is a (perhaps degenerate) geodesic curve of Σ_t. This curve is also a spacelike (or else degenerate) geodesic curve of the full space–time manifold $\mathfrak{M}$, and σ measures proper distance along it.

From Eqs. (50) and (55) it follows that $\dot{\sigma}^2 = k^2 - \epsilon$, hence that $\ddot{\sigma} = 0$. Thus test particles undergo no accelerations of the classical Newtonian kind that are associated with forces. In this sense the manifold $\mathfrak{M}$ produces no gravitational effects on test particles (or on light rays, for that matter), and $\mathfrak{M}$ can therefore be said to be devoid of gravitating mass. This, however, is not to say that $\mathfrak{M}$ is free of all matter. The reason for not ruling out massless matter is that in $\mathfrak{M}_{0,n}$ all nonradial test particle or light ray paths bend toward the drainhole, even to the extent that many of them loop around it again and again. This will become apparent as next the geodesics of $\mathfrak{M}_{0,n}$ are described in detail.

It is sufficient to consider in $\mathfrak{M}_{0,n}$ those spacelike geodesic paths p for which $\dot{t} = k = 0$, inasmuch as all geodesics project onto them in the manner described above; these are just the geodesic paths of Σ_t with respect to the inherited Riemannian line element (3), parametrized by arc length. It is further sufficient to consider the case where $\vartheta = \pi/2$, and then p will lie on the catenoid depicted in Fig. 1. On some of these geodesics $\rho \equiv 0$ and $\dot{\varphi}^2 = 1/n^2$. On all others any zero that $\dot{\rho}$ has must be isolated, and for these Eqs. (49) and (52) can be combined into the orbital equation

$$\left(\frac{d\varphi}{d\rho}\right)^2 \equiv \left(\frac{\dot{\varphi}}{\dot{\rho}}\right)^2 = \frac{h^2}{r^2(r^2 - h^2)} = \frac{h^2}{(\rho^2 + n^2)(\rho^2 + n^2 - h^2)}, \tag{57}$$

valid except at isolated points of the path p.

The geodesics fall naturally into three classes, corresponding to (a) $h^2 > n^2$, (b) $h^2 = n^2$, and (c) $h^2 < n^2$. Typical and atypical geodesics in these classes are shown in Fig. 6. Each of them reflects through the drainhole onto a geodesic of the same class.

A typical geodesic satisfying $h^2 > n^2$ spirals in from infinity to a minimum distance $(h^2 - n^2)^{1/2}$ from the neck of the drainhole (where $\rho = 0$), and then spirals out to infinity again. The smaller the distance of closest approach to the neck of the drainhole, the greater the

number of revolutions around the drainhole. A test particle on such an orbit can be trapped for any length of time (whether coordinate time t or proper time τ), but ultimately it will escape. There are no atypical geodesics in this class.

If $h^2 = n^2$, a typical geodesic orbit starts from infinity and spirals in asymptotically to the center circle, which itself is the lone atypical geodesic orbit for this case. A test particle on one of these orbits will be trapped forever, or, if it follows the orbit in reverse, has been trapped forever but is gradually escaping.

In case $h^2 < n^2$, a typical geodesic spirals in from infinity, passes through the drainhole, and spirals out to infinity on the other side. The atypical geodesics trace out the ρ lines, which pass through the hole but do not spiral. Test particles following these orbits are lost forever to observers on the initial side, who would be able, however, upon looking toward the drainhole, to see them slowly fading away, like scintillations in a crystal ball.

The capturing of test particles and of light rays by the flowless drainhole for various lengths of time ranging upward to infinity would seem to warrant thinking of the manifold $\mathfrak{M}_{0,n}$ as at least a rudimentary model of what a massless nuclear binding particle might be like. One's inclination in this direction is reinforced by the observation that the capture effect is of short range. For example, if the distance of closest approach is 10 times the drainhole radius n, then the total bending of the geodesic amounts to less than $0.5°$. For the total bending to be $180°$ (half a loop), the distance of closest approach must be about $0.2n$, which puts the point of closest approach on a sphere of symmetry whose radius is about $1.02n$; for a full loop the corresponding numbers are about $0.03n$ and $1.0006n$.

Geodesics of $\mathfrak{M}_{m,n}$ $(m > 0)$

The discussion will proceed mainly from Eq. (52), rewritten as

$$\dot{\rho}^2 = 2E + F_\epsilon(h^2, \rho), \tag{58}$$

where $E = \frac{1}{2}(k^2 - \epsilon)$ and

$$F_\epsilon(h^2, \rho) = \epsilon f^2 - h^2(1 - f^2)/r^2$$
$$= \epsilon[1 - e^{-(2m/n)\alpha(\rho)}] - h^2/e^{(4m/n)\alpha(\rho)}(\rho^2 + a^2)^1. \tag{59}$$

An adequate qualitative description of the geodesics can be easily read off from the graphs, for $\epsilon = 0, 1, -1$, of the functions of the family $F_\epsilon(h^2, \rho)$. Because $\ddot{\rho} = \frac{1}{2}F_\epsilon'(h^2, \rho)$, the turning points of orbits will occur where $F_\epsilon(h^2, \rho) = -2E$ and $F_\epsilon'(h^2, \rho) \neq 0$, and circular orbits will occur where $F_\epsilon(h^2, \rho) = -2E$ and $F_\epsilon'(h^2, \rho) = 0$. The circular orbits will be stable if $F_\epsilon''(h^2, \rho) < 0$, unstable if $F_\epsilon''(h^2, \rho) > 0$.

Null geodesics

Here $2E = k^2 \geq 0$. The graphs of the functions $F_0(h^2, \rho)$ appear in Fig. 7. Adding $2E$ to $F_0(h^2, \rho)$ to get $\dot{\rho}^2$ shifts the graphs upward (unless $2E = 0$); only those points of the graphs that are shifted to the upper closed half-plane correspond to points of geodesics. For various ranges of E and h^2 the possibilities can be summarized as follows:

(i) $E = 0$:

(a) $h^2 = 0$; degenerate geodesic at each point of $\mathfrak{M}_{m,n}$.

(b) $h^2 > 0$; no geodesic.

(ii) $E > 0$:

(a) $0 \leq h^2 < 2Er^2(2m)[1 - f^2(2m)]^{-1}$; geodesics beginning at ∞, passing through the drainhole, ending at $-\infty$, and vice versa.

(b) $h^2 = 2Er^2(2m)[1 - f^2(2m)]^{-1}$; geodesics with unstable circular orbit at $2m$; geodesics beginning at ∞
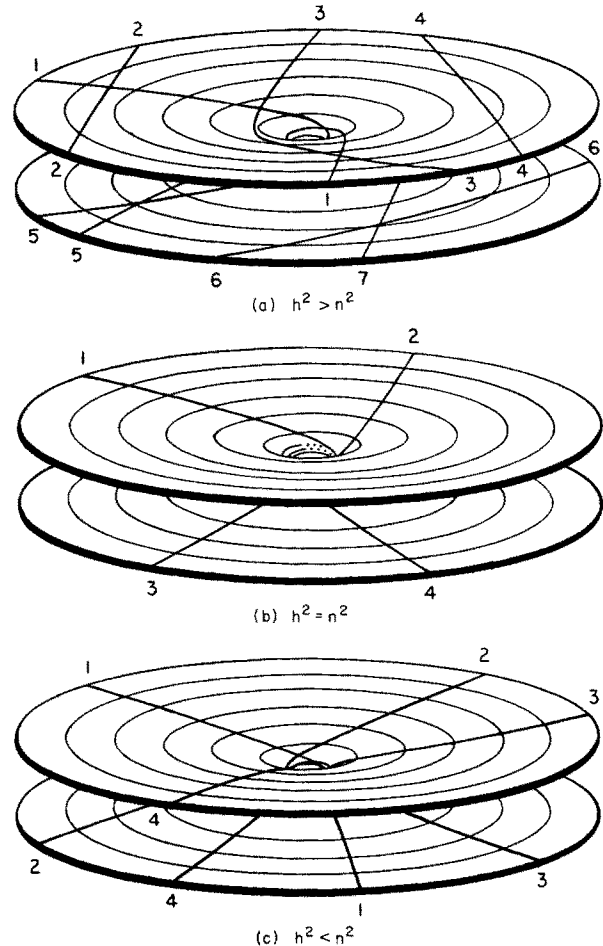

FIG. 6. Typical and atypical orbits of test particles (a) around, (b) about, and (c) through the drainhole of Case III $(n^2 < m^2)$ when $m = 0$. The surface to which the orbits are confined is the catenoid of Fig. 1. It is isometric to every great-circle cross section of the spherically symmetric space surrounding the drainhole. The orbits fall into the three classes according to the amount h of angular momentum. The only atypical orbits are the central circle in (b) and the radial lines in (c). Every reflection of an orbit in the drainhole is again an orbit of the same class.
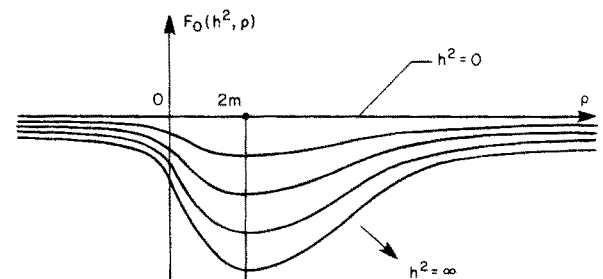

FIG. 7. The graphs of the functions $F_0(h^2, \rho)$ for various values of h^2. Each function has a minimum at $2m$. From the equation $\dot{\rho}^2 = 2E + F_0(h^2, \rho)$ one can find the turning points of null geodesics of $\mathfrak{M}_{m,n}$ by referring to this picture.

and ending by spiraling down to the circular orbit, and vice versa, spiraling up from the circular orbit to ∞; geodesics beginning at $-\infty$, passing through the drainhole, and ending by spiraling up to the circular orbit, and vice versa.

(c) $h^2 > 2Er^2(2m)[1 - f^2(2m)]^{-1}$; geodesics beginning and ending at ∞, reaching lowest points (ρ a minimum) which move up from just above $2m$ to ∞ as E decreases or h^2 increases; geodesics beginning and ending at $-\infty$, reaching highest points (ρ a maximum) which move down from just below $2m$ to $-\infty$ as E decreases or h^2 increases.

Timelike geodesics

In this case $2E = k^2 - 1 \geq -1$. Figure 8 exhibits the graphs of the functions $F_1(h^2, \rho)$. Their critical points occur where $h^2 = mr^2(\rho)(\rho - 2m)^{-1} \equiv \gamma(\rho)$, which is on the upper side of $2m$. The locus of critical points has a maximum where $\rho = 3m + (4m^2 + n^2)^{1/2} \equiv \rho_0$, and a zero, ρ_1, between $2m$ and ρ_0. The catalog of timelike geodesics reads as follows:

(i) $-1 \leq 2E \leq 1 + e^{-(2m\pi/a)}$: no geodesic.

(ii) $-1 + e^{-(2m\pi/a)} < 2E < -F_1(\gamma(\rho_0), \rho_0)$:

(a) $0 \leq h^2 < \gamma(\rho_0)$; geodesics beginning and ending at $-\infty$, reaching highest points (ρ a maximum) which move from above ρ_0 down to $-\infty$ as E decreases.

(b) $h^2 \geq \gamma(\rho_0)$; geodesics beginning and ending at $-\infty$, reaching highest points below ρ_0 which move down to $-\infty$ as E decreases or h^2 increases.

(iii) $2E = -F_1(\gamma(\rho_0), \rho_0)$:

(a) $0 \leq h^2 < \gamma(\rho_0)$; geodesics beginning and ending at $-\infty$, reaching highest points above ρ_0.

(b) $h^2 = \gamma(\rho_0)$; geodesics with semistable circular orbit at ρ_0 [small perturbations satisfying $2(E + \Delta E) + F_1(h^2 + \Delta h^2, \bar{\rho}) \leq 0$, where $\bar{\rho}$ is the lesser root of $\gamma(\rho) = h^2 + \Delta h^2$, change the orbit but little, and all other small perturbations result in orbital decay to $-\infty$]; geodesics beginning at $-\infty$ and ending by spiraling up to the circular orbit, and vice versa, spiraling down from the circular orbit to $-\infty$.

(c) $h^2 > \gamma(\rho_0)$; geodesics beginning and ending at

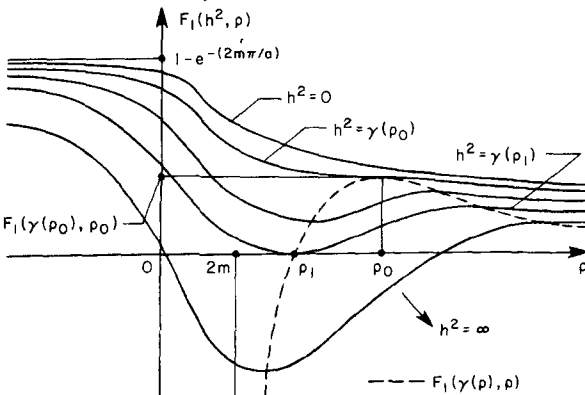

FIG. 8.   The graphs of the functions $F_1(h^2, \rho)$ for various values of h^2. The dashed curve is the locus of critical points of the functions, which are minima to the left of, maxima to the right of $\rho_0[= 3m + (4m^2 + n^2)^{1/2}]$. $F_1(\gamma(\rho_0), \rho)$ has a horizontal inflection point at ρ_0. As $\rho \to -\infty, F_1(h^2, \rho) \to 1 - e^{-(2m\pi/a)}$. As $\rho \to 2m+, F_1(\gamma(\rho), \rho) \to -\infty$. As $\rho \to \infty, F_1(h^2, \rho) \to 0$ and $F_1(\gamma(\rho), \rho) \to 0$. From the equation $\dot{\rho}^2 = 2E + F_1(h^2, \rho)$ one can find the turning points of timelike geodesics of $\mathfrak{M}_{m,n}$ by referring to this picture.

$-\infty$, reaching highest points which move from just below ρ_0 down to $-\infty$ as E decreases or h^2 increases.

(iv) $-F_1(\gamma(\rho_0), \rho_0) < 2E < 0$. Let ρ^* and ρ^{**} denote the two roots of $2E + F_1(\gamma(\rho), \rho) = 0$, with $\rho^* < \rho^{**}$; let $\bar{\rho}^*$ denote the root of $2E + F_1(\gamma(\rho^*), \rho) = 0$ distinct from ρ^*, and define $\bar{\rho}^{**}$ analogously. Then $\bar{\rho}^{**} < \rho^* < \rho_0 < \rho^{**} < \bar{\rho}^*$, and, as E increases, ρ^* moves down from ρ_0- to ρ_1+, while ρ^{**} moves up from ρ_0+ to ∞.

(a) $0 \leq h^2 < \gamma(\rho^*)$; geodesics beginning and ending at $-\infty$, reaching highest points above $\bar{\rho}^*$.

(b) $h^2 = \gamma(\rho^*)$; geodesics with unstable circular orbit at ρ^*; geodesics beginning at $-\infty$, passing through the drainhole, and ending by spiraling up to the circular orbit, and vice versa; geodesics beginning by spiraling up from the circular orbit to highest points at $\bar{\rho}^*$, ending by spiraling back down to the circular orbit.

(c) $\gamma(\rho^*) < h^2 < \gamma(\rho^{**})$; geodesics beginning and ending at $-\infty$, reaching highest points between $\bar{\rho}^{**}$ and ρ^*; geodesics having stable bound orbits and periodic radial motions, with lowest points between ρ^* and ρ^{**} and highest points between ρ^{**} and $\bar{\rho}^*$.

(d) $h^2 = \gamma(\rho^{**})$; geodesics beginning and ending at $-\infty$, reaching highest points at $\bar{\rho}^{**}$; geodesics with stable circular orbit at ρ^{**}.

(e) $h^2 > \gamma(\rho^{**})$; geodesics beginning and ending at $-\infty$, reaching highest points below $\bar{\rho}^{**}$ which move down to $-\infty$ as h^2 increases.

(v) $2E \geq 0$. Let ρ^* be the root of $2E + F_1(\gamma(\rho), \rho) = 0$. As E increases, ρ^* moves down from ρ_1 to $2m+$.

(a) $0 \leq h^2 < \gamma(\rho^*)$; geodesics beginning at ∞, passing through the drainhole, ending at $-\infty$, and vice versa.

(b) $h^2 = \gamma(\rho^*)$; geodesics with unstable circular orbit at ρ^*; geodesics beginning at ∞, ending by spiraling down to the circular orbit, and vice versa; geodesics beginning at $-\infty$, passing through the drainhole, ending by spiraling up to the circular orbit, and vice versa.

(c) $h^2 > \gamma(\rho^*)$; geodesics beginning and ending at ∞, reaching lowest points which move up from just above ρ^* to ∞ as h^2 increases; geodesics beginning and ending at $-\infty$, reaching highest points which move down from just below ρ^* to $-\infty$ as h^2 increases.

Spacelike geodesics

When one examines the graphs (not presented here) of the functions $F_{-1}(h^2, \rho)$, taking into account that $2E = k^2 + 1 \geq 1$, he sees that the spacelike geodesics fall into three classes analogous to the three classes of timelike geodesics on which $2E \geq 0$. The principle observation of interest is that, as E increases, the circular orbits move up from m, where the drainhole is narrowest, to just below $2m$.

Capture of light rays and test particles

With good enough starts both light rays and test particles can coast upstream all the way to ∞, even if they begin as far down as $-\infty$ and procrastinate by spiraling as they go. The drainhole, then, is no "black hole" like the Schwarzschild singularity, surrounded by its one-way horizon. On the other hand, the drainhole does absorb many of the light rays and test particles that approach it from the upper side, by either capturing them or letting them pass through to the lower side. Perhaps the drainhole would qualify as a "gray hole."

For the Schwarzschild model with positive mass m' Darwin has established that no test particle orbit can have its pericenter as low as $3m'$.[19] The analogous proposition is true for the drainhole model: No such orbit has its lowest point or points as low as $2m$. Another aspect of the drainhole geodesics is that, although there are unstable, bound (actually circular), test particle orbits at ρ_0 and below, every such orbit that is stable must have its highest points above ρ_0 and its energy E greater than $-\frac{1}{2} F_1(\gamma(\rho_0), \rho_0)$. This property, reminiscent of a salient feature of quantum mechanical models of the hydrogen atom, also finds an analog in the Schwarzschild model.[19] It is worth noting that neither of these common properties depends upon the presence of a horizon, as the Schwarzschild manifold suggests it might.

In the Schwarzschild model the spatial cross sections Σ_t are flat, and the capture effects can be attributed to the gravitational field alone. In the drainhole model, however, some of the credit must go to the curvature of space around the drainhole, for, as we have seen, the effects persist, at short range, even when the gravitational field vanishes. Thus the drainhole with the flowing ether can be thought of as a first approximation to a geometrical model of a massive nuclear binding particle. On the other hand, one can use it in place of the Schwarzschild manifold to model the gravitational field of, for example, the sun. In this connection one can calculate that at large distances from the drainhole the bending of orbits caused by the curvature of space results in an increase in the precessions of orbital perihelia that is of higher infinitesimal order than the precessions themselves. This correction to the precessions differs both in order of magnitude and in sense from the corresponding correction in the Brans–Dicke scalar–tensor theory.[20]

IX. DISCUSSION

In the field equation (26), which the ether-flow, drainhole, particle model satisfies, the polarity of the coupling between the geometry of space–time and the scalar field is reversed from that which most physicists accept. I shall therefore review here some arguments in support of it, as well as one argument against it.

Justification of the coupling must rest ultimately on the reasonableness and usefulness that the space–time manifolds derivable from it possess as models of the physical world. The ether-flow, drainhole model derived from it has in common with the Schwarzschild manifold the useful ability to reproduce to within current observational tolerances the external gravitational field of a massive, nonrotating, spherically symmetric body. It does not have the Schwarzschild manifold's useless point singularity or the associated and equally useless incompleteness of geodesics. It also, reasonably if not usefully, has no horizon. In place of these dubious endowments it has several novelties of its own, whose reasonableness or unreasonableness, usefulness or unusefulness are yet to be determined. It ties together as two aspects of one entity the concept of negative (active) gravitational mass and that of positive,[21] at the same time hinting at a universal excess of the negative over the positive, in a ratio involving Dirac's outsized numbers. It stands as a clear indicator that within geometrodynamics, to use Wheeler's descriptive term for general relativity theory,[5] there is room at least for classical models of nuclear binding

particles, with mass and without, if one will but relax the field equations enough to allow static negative curvatures of space. Finally, the drainhole suggests a dynamically topological mechanism for the dematerialization of such particles into traveling ripples in the fabric of space and also, because of time reversal symmetry, for their materialization out of these ripples.

Historically, Einstein took the coupling constant K in his field equations

$$R_{\mu\nu} - \tfrac{1}{2} R g_{\mu\nu} = K T_{\mu\nu} \qquad (60)$$

to be negative in order to satisfy the requirement that in the quasistatic, weak-field approximation these equations should approximate the content of the Poisson equation for the Newtonian gravitational potential V, an equation which reads $\nabla^2 V = 4\pi(\rho_M + \rho_E)$, where ρ_M is the density of mass and ρ_E the density of any other forms of energy that are thought to cause gravitational phenomena.[22] Einstein carried through his argument, however, only for the case in which the energy–momentum tensor components $T_{\mu\nu}$ arise solely from slowly moving dust of small but nonzero proper density, for which case $\rho_M \neq 0$ and $\rho_E = 0$. If in the other extreme $(\rho_M = 0, \rho_E \neq 0)$ the only energy present is embodied in a scalar field ϕ of rest mass zero, associated with the Lagrangian density $(-g)^{1/2} \phi^{,\kappa} \phi_{,\kappa}$, then

$$T_{\mu\nu} = \phi_{,\mu} \phi_{,\nu} - \tfrac{1}{2} \phi^{,\kappa} \phi_{,\kappa} g_{\mu\nu}, \qquad (61)$$

and Eq. (60) is equivalent to

$$R_{\mu\nu} = K \phi_{,\mu} \phi_{,\nu}. \qquad (62)$$

In the quasistatic, weak-field approximation $V \approx \frac{1}{2}(g_{00} - 1)$, $R_{00} \approx -\nabla^2 V$, and $\phi_{,0}\phi_{,0} \approx 0$. Thus the Poisson equation whose content is approximated by $R_{00} = K\phi_{,0}\phi_{,0}$ is actually the Laplace equation $\nabla^2 V = -K \cdot 0$. The other field equations approximate to $0 = K \cdot 0$. Therefore, the requirement of correspondence with Newtonian theory yields in this case no information about K.

The failure of the correspondence requirement to fix the polarity of the scalar-field coupling leaves one free to apply other criteria to the task. It has seemed to me quite reasonable to eschew singularities and aim at a theory that will provide as a model for a mass particle at rest and alone in the universe a static space–time manifold that is geodesically complete and is asymptotic to a Schwarzschild manifold with nonzero mass parameter.[23] This criterion forces K to be positive in the variational principle (25), by way of the following argument.

Let us first take notice that every static and spherically symmetric line element is a special case of the line element (1). Indeed, every such line element can by a coordinate transformation be brought locally into the form

$$d\tau^2 = A(R)dT^2 - B(R)dR^2 - C^2(R)d\Omega^2, \qquad (63)$$

with $A, B,$ and C positive. Then a further transformation, changing only the radial coordinate, will take it to the form (1_S). The latter transformation is obtained by solving the differential equation $dR/d\rho = [A(R)B(R)]^{1/2}$ for R as an increasing, therefore invertible function of the new coordinate ρ. Finally, by using Eq. (21) in reverse, we can arrive at the form in Eq. (1).

Now let us recall that the discussion in Secs. VII and VIII established that if $\phi = \alpha(\rho)$, then the Euler equations associated with the variational principle (25) have the drainhole manifold as their only solution manifold that has a line element of the form (1), is geodesically complete, and is asymptotic to a Schwarzschild manifold with nonzero mass parameter, and, further, the drainhole is a solution only if $K > 0$. Finally, if $\phi = \alpha(t, \rho, \vartheta, \varphi)$, then one can without great difficulty see that the Euler equations imply that in fact ϕ depends only upon ρ, hence that the foregoing conclusion applies also in this case. To summarize, then, if and only if $K > 0$ does there exist a static, geodesically complete, and spherically symmetric space–time manifold that is asymptotic to a Schwarzschild manifold with nonzero mass parameter and that satisfies the variational principle (25) for some choice of the scalar field ϕ, and the drainhole manifold, with its numerous interesting and useful features, is the one.

Against the advantages that I have set forth for the nonstandard choice of coupling polarity one must array whatever implications it has that seem to be in disagreement with established theory. The only such implication that I have met is this: According to conventional interpretation, the scalar field, when coupled with nonstandard polarity to the geometry of space–time, must be accounted as having negative energy, contrary to the usual requirement of general relativity theory.[24] Specifically, with $K > 0$ one would say, following the usual convention, that the energy density of the scalar field is $-T_{00}$ as given in a physically significant reference frame by Eq. (61). Because T_{00} is positive definite in physically significant reference frames, such as local Lorentz frames, the energy density $-T_{00}$, hence also the total energy of the scalar field, would be negative definite. Perhaps this interpretation is correct. I have to confess that I have been unable to conclude or to be persuaded that the polarity of the coupling between a nonmaterial field and the geometry of space–time should determine or be determined by the positiveness or negativeness of the energy of that field. I prefer to postpone the question, looking forward to the day when we shall have a satisfactory, nonphenomenological unified field theory in which there appear no coupling constants whose polarity has to be assigned.

It is instructive to compare the scalar-field energy E_S in the drainhole model, be it positive or be it negative, with the energy E_G of the gravitational field. I take E_G to be the mass m, thereby remaining consistent with the view expressed in Sec. III and again in Sec. VIII that true gravity is generated only by internal motions of the ether and therefore vanishes when $f = 0$ (equivalently, when $m = 0$). For definiteness let us assume that $E_S \geq 0$. Then, after normalization by the conventional factor $(4\pi)^{-1}$,

$$E_S = (1/4\pi)\int_\Sigma T_{00}(-\det g_{mn})^{1/2}d^3x, \tag{64}$$

where Σ is a hyperspace orthogonal to the timelike Killing vector field $\partial/\partial T$, and $[x^\mu] = [T, \rho, \vartheta, \varphi]$, the form of the line element being therefore that in Eq. (1_S). Upon calculation of T_{00} and subsequent application of Eqs. (43), we have

$$E_S = \frac{1}{4\pi}\int_{-\pi}^\pi \int_0^\pi \int_{-\infty}^\infty \tfrac{1}{2}[(1-f^2)\alpha']^2$$

$$\times r^2(\sin\vartheta)(1-f^2)^{1/2}d\rho\, d\vartheta\, d\varphi$$

$$= \begin{cases} \dfrac{n\pi}{2} & \text{if } m = 0, \\[2ex] \dfrac{n^2}{2m}\left[1 - \exp\left(\dfrac{-m\pi}{(n^2-m^2)^{1/2}}\right)\right] & \text{if } m > 0. \end{cases} \tag{65}$$

One sees that, as m increases from 0 to n, E_S decreases continuously from $n\pi/2$ to $n/2$. Hence the amount of energy in the scalar field is essentially proportional to n, regardless of the amount m of gravitational energy, and it actually varies inversely with m. If $m \ll n$, then $E_S/E_G \approx n\pi/2m$. In the case of the numbers mentioned in Sec. VII, where m was approximately the mass of a proton, $E_S/E_G \approx 10^{19}$ if n is of the order of Planck's length, and $E_S/E_G \approx 10^{39}$ if n is near the classical electron radius. Here are two more occurrences of the ubiquitous Dirac numbers.[18] The large sizes of these ratios demonstrate that the scalar field (more generally, the curvature of space) is a promising agent for representing within general relativity theory natural phenomena much more energetic than gravity and having to do with particles of subatomic size.

ACKNOWLEDGMENTS

APPENDIX

This is a brief outline of the computational framework used in the body of the paper. The approach is that of Cartan.[25]

On the differentiable manifold $\mathfrak{M}$ the tangent vectors at the point P are thought of as those local differential operators on the scalar fields differentiable at P that for some coordinate system $[x^\mu]$ at P are linear combinations of the operators $(\partial/\partial x^\mu)(P)$. The tangent space at P is denoted by T^P and its dual, the space of tangent covectors at P, or cotangent space at P, by T_P. The basis of T_P dual to the basis $\{(\partial/\partial x^\mu)(P)\}$ of T^P is denoted by $\{dx^\mu(P)\}$. After an obvious pattern the elements of the various tensor product spaces, such as $T_P \otimes T_P$, $T_P \otimes T^P$, $T_P \otimes T_P \otimes T^P$, are distinguished among by use of the names cocotensor, cocontensor, cococontensor, and so on. The elements of T_P, $T_P \wedge T_P$, $T_P \wedge T_P \wedge T_P$, $\cdots$ are the 1-, 2-, 3-, $\cdots$ forms.

The connection forms of the covariant differentiation (affine connection) d on $\mathfrak{M}$, with respect to the frame system $\{e_\mu\}$ and its dual $\{\omega^\mu\}$, are the 1-forms $\{\omega_\mu{}^\kappa\}$ determined by either of the equations

$$de_\mu = \omega_\mu{}^\kappa \otimes e_\kappa \tag{A1}$$

and

$$d\omega^\mu = -\omega_\kappa{}^\mu \otimes \omega^\kappa. \tag{A2}$$

If $p : I \to \mathfrak{M}$ is a path in $\mathfrak{M}$, I being its parameter interval, and u is a vector field on p (that is to say, u is a function on I, and $u(t) \in T^{p(t)}$ for each t), then $\dot{u}$, the covariant derivative of u, is computed from

$$\dot{u} = [u^\mu e_\mu(p)]^{\cdot} = \dot{u}^\mu e_\mu(p) + u^\mu de_\mu(p)\dot{p}$$

$$= [\dot{u}^\kappa + u^\mu \omega_\mu{}^\kappa(p)\dot{p}]e_\kappa(p). \tag{A3}$$

Let d_e be the exterior covariant differentiation based on d, defined by saying that, for every co...co- or co...

cocontensor field V on $\mathfrak{M}$, $d_e V$ is the totally skew-symmetric part of dV. Then the torsion of $\mathbf{d}$ is the skew-symmetric cococontensor field T uniquely determined by the requirement that if v is a covector field, then

$$dv - \mathbf{d}_e v = vT, \tag{A4}$$

where d stands for (noncovariant) exterior differentiation and where juxtaposition means composition, e.g., $(vT)(u_1, u_2) = v(T(u_1, u_2))$. The curvature tensor field is the unique cococontensor field Θ that is skew-symmetric in the second and third slots and satisfies

$$\mathbf{d}_e^2 u = \Theta u - (du)T \tag{A5}$$

for every vector field u. In terms of $\{e_\mu\}$ and $\{\omega^\mu\}$,

$$\Theta = \omega^\kappa \otimes \Theta_\kappa{}^\mu \otimes e_\mu, \tag{A6}$$

the curvature 2-forms $\Theta_\kappa{}^\mu$ being given by

$$\begin{aligned}\Theta_\kappa{}^\mu &= d\omega_\kappa{}^\mu - \omega_\kappa{}^\lambda \wedge \omega_\lambda{}^\mu\\&= -\tfrac{1}{2}R_\kappa{}^\mu{}_{\lambda\nu}(\omega^\nu \wedge \omega^\lambda),\end{aligned} \tag{A7}$$

where the $R_\kappa{}^\mu{}_{\lambda\nu}$ are the components of the Riemann–Christoffel curvature tensor field ($\equiv -2\Theta$). If $d\omega^\mu = C_\kappa{}^\mu{}_\lambda(\omega^\lambda \wedge \omega^\kappa)$, and $\omega_\kappa{}^\mu = \Gamma_\kappa{}^\mu{}_\lambda \omega^\lambda$, then

$$R_\kappa{}^\mu{}_{\lambda\nu} = 2(\Gamma_\kappa{}^\mu{}_{[\nu,\lambda]} + \Gamma_\kappa{}^\rho{}_{[\nu}\Gamma_{|\rho|}{}^\mu{}_{\lambda]} + \Gamma_\kappa{}^\mu{}_\rho C_{[\nu}{}^\rho{}_{\lambda]}). \tag{A8}$$

Here $C_{[\kappa}{}^\mu{}_{\lambda]} = \tfrac{1}{2}(C_\kappa{}^\mu{}_\lambda - C_\lambda{}^\mu{}_\kappa)$, and similarly for other square-bracketed pairs of indices. Contracting Θ in the second and fourth slots produces the contracted curvature tensor field Φ:

$$\Phi = \omega^\kappa \otimes \Theta_\kappa{}^\mu e_\mu = \omega^\kappa \otimes (-\tfrac{1}{2}R_{\kappa\lambda}\omega^\lambda), \tag{A9}$$

where $R_{\kappa\lambda} \equiv R_\kappa{}^\mu{}_{\lambda\mu}$, the components of the Ricci curvature tensor field ($\equiv -2\Phi$).

If $\mathbf{d}$ is required to be consistent with a metric G (any global, nondegenerate, symmetric cocotensor field on $\mathfrak{M}$), in the sense that $\mathbf{d}G = 0$, and to have torsion T (any global, skew-symmetric cococontensor field on $\mathfrak{M}$, given a priori), then $\mathbf{d}$ is uniquely determined. With respect to an orthonormal frame system $\{e_\mu\}$ and its dual $\{\omega^\mu\}$, the connection forms of $\mathbf{d}$ are easy to calculate using an algorithm of Misner.[26] It consists in solving for $[\omega_\kappa{}^\mu]$ the matrix equation

$$[\omega^\kappa] \wedge [\omega_\kappa{}^\mu] = [(C_\kappa{}^\mu{}_\lambda - T_\kappa{}^\mu{}_\lambda)(\omega^\lambda \wedge \omega^\kappa)], \tag{A10}$$

where $T = T_\kappa{}^\mu{}_\lambda(\omega^\lambda \wedge \omega^\kappa \otimes e_\mu)$, utilizing the symmetries and antisymmetries implied by $\omega_\mu{}^\kappa g_{\kappa\nu} + \omega_\nu{}^\kappa g_{\kappa\mu} = dg_{\mu\nu} = 0$. It is easiest to do this individually for each nonzero term on the right and then add the results.

[1] K. Schwarzschild, S.-B. Preuss, Akad. Wiss, Phys.-Math. K1. 7, 189 (1916).

[2] A. Einstein and N. Rosen, Phys. Rev. 48, 73 (1935).

[3] M. D. Kruskal, Phys. Rev. 119, 1743 (1960).

[4] C. Fronsdal, Phys. Rev. 116, 778 (1959).

[5] J. A. Wheeler, Geometrodynamics (Academic, New York, 1962).

[6] G. D. Birkhoff, Relativity and Modern Physics (Harvard U.P., Cambridge, Mass., 1923), p. 253.

[7] The symbol t is now overloaded, representing both coordinate function and constant. Such ambiguities are to be resolved by appeal to context.

[8] Here the argument ρ is suppressed for convenience's sake. It will be suppressed again on occasion.

[9] Einstein was convinced that the luminiferous ether, driven out of physicists' thoughts by the special theory of relativity, had returned as an essential feature of the general theory, intimately involved with gravity and only secondarily if at all connected with electromagnetism. He did not, however, recognize in it any degree of substantiality or of motility. In his essay "Relativity and the Ether" he wrote: "According to the general theory of relativity space is endowed with physical qualities; in this sense, therefore, an ether exists. In accordance with the general theory of relativity space without an ether is inconceivable.... But this ether must not be thought of as endowed with the properties characteristic of ponderable media, as composed of particles the motion of which can be followed; nor may the concept of motion be applied to it." [A. Einstein, Essays in Science, translated by A. Harris (Philosophical Library, New York, 1934).]

[10] Anyone willing to consider the ether-flow hypothesis as plausible might wish to ask whether, if the earth is conceivably a conglomeration of ether sinks and sources, the conventional interpretation of the Michelson–Morley experiment ought not to be revised.

[11] W. de Sitter, Proc. K. Ned. Akad. Wet. 19, 1217 (1917); Proc. K. Ned. Akad. Wet. 20, 229 (1917).

[12] A. Trautman has found before now that the Schwarzschild and the de Sitter line elements can be cast in the form (1). He has also applied the term "the ether" in these instances, but in a way that precludes any attribution of substantiality to the ether. [Perspectives in Geometry and Relativity, Essays in Honor of Václav Hlavatý, edited by B. Hoffman (Indiana U.P., Bloomington, 1966), p. 413.]

[13] One could raise the point that the Schwarzschild manifold, which satisfies Eq. (24) no matter what the coupling constant K (just let ϕ be a constant), already has a central hole, the "wormhole" of the Kruskal–Fronsdal extension. This hole, however, is not a permanent feature of the spatial cross sections; it develops into the Schwarzschild singularity when pursued in either temporal direction. Although at this point I have not said it in so many words, I have in mind that the particle models I seek shall be static, which alone would rule out the Schwarzschild manifold, even without the completeness requirement. One might also wish to say that a Schwarzschild interior solution, properly matched to an exterior solution, would provide a model of just the kind I want, without even introducing the scalar field ϕ. I would have to reply that such a manifold can only represent a mass body, not a particle. To electromagnetic geons as particle models (J. A. Wheeler, Ref. 5) my foremost objection would be that they are not static.

[14] A. I. Janis, E. T. Newman, and J. Winicour, Phys. Rev. Lett. 20, 878 (1968).

[15] R. Penney, Phys. Rev. 174, 1578 (1968).

[16] O. Bergmann and R. Leipnik, Phys. Rev. 107, 1157 (1957). In fact these authors formulated the full set of solutions under discussion here. However, they ruled out for "physical reasons" the very case to which I attach the greatest physical significance, Case III. Handicapped by a restrictive coordinate system, they nevertheless were able to identify most parts of the solution manifolds in Cases I and II.

[17] H. Yilmaz, Introduction to the Theory of Relativity and the Principles of Modern Physics (Blaisdell, New York, 1965), p. 176. The $R_{\kappa\lambda}$ used by Yilmaz are the negatives of those appearing here. This has the consequence that his Eq. (18.2), although seemingly equivalent to the present Eq. (26), actually involves the coupling of opposite polarity and therefore is not satisfied by his line element (18.3) unless ϕ is constant. See also H. Yilmaz, Phys. Rev. 111, 1417 (1958).

[18] P. A. M. Dirac, Proc. R. Soc. Lond. 165, 199 (1938); Nature (Lond.) 139, 323 (1937).

[19] C. Darwin, Proc. R. Soc. A 249, 180 (1959).

[20] C. Brans and R. H. Dicke, Phys. Rev. 124, 925 (1961).

[21] These concepts are also combined, in a somewhat analogous fashion, in the Kerr solution of the Einstein vacuum field

equations. [B. Carter, Phys. Rev. **174**, 1559 (1968).]

[22]A. Einstein, Ann. Phys. (Leipz.) **49**, 769 (1916), or see *The Principle of Relativity* (Dover, New York, 1923), p. 157.

[23]There is an earlier instance in which to meet a new criterion the polarity of the coupling in Eq. (60) was partially reversed. Einstein and Rosen reversed it for the coupling of space–time geometry to the electromagnetic field in order to represent an elementary charged mass particle as one of their "bridges" (A. Einstein and N. Rosen, Ref. 2).

[24]At the Relativity Conference in the Midwest, Cincinnati, Ohio, June 2–6, 1969, István Ozsváth was good enough to raise and to discuss with me this issue. Also, the referee has pressed it upon me in a friendly manner. The referee's argument, based upon energy conservation, is persuasive but not, to my mind, conclusive. For this reason I shall not recapitulate it here; neither shall I at the end profess to have resolved the issue

[25]É. Cartan, *Leçons sur la géométrie des espaces de Riemann* (Gauthier-Villars, Paris, 1946), 2nd ed. See also H. Flanders, *Differential Forms with Applications to the Physical Sciences* (Academic, New York, 1963), and R. L. Bishop and S. I. Goldberg, *Tensor Analysis on Manifolds* (Macmillan, New York, 1968).

[26]C. W. Misner, J. Math. Phys. **4**, 924 (1963).